

1. High velocity flow jet in an up-stream stenosis in the transverse sinus directed at the SSD opening,
2. Flow jet into the SSD along the long axis of the SSD, either anteriorly or laterally directed,
3. Vortex of flow in the SSD,
4. Prominent vortex component of flow in the sigmoid sinus downstream from SSD,
5. Vortex of flow in the jugular bulb

Three of the patients had simulated post-coil treatment models developed excluding the SSD from the models. CFD showed no flow in SSD and decreased vortex component of flow in the sigmoid sinus downstream from the SSD.

Conclusion PT caused by SSD may be caused by a unique flow pattern in the SSD and sinuses as visualized on both MRV and CFD.

Disclosures M. Amans: None. E. Kao: None. S. Kefayati: None. K. Meisel: None. F. Faraji: None. C. Glastonbury: None. M. Ballweber: None. V. Halbach: None. D. Saloner: None.

0-033 JUGULAR VEIN FLOW PATTERNS IN PATIENTS WITH PULSATILE TINNITUS USING COMPUTATIONAL FLUID DYNAMICS

¹E Kao, ¹S Kefayati, ²K Meisel, ¹M Ballweber, ¹F Faraji, ¹V Halbach, ¹D Saloner, ¹M Amans. ¹Radiology, UCSF, San Francisco, CA; ²Neurology, UCSF, San Francisco, CA

10.1136/neurintsurg-2016-012589.33

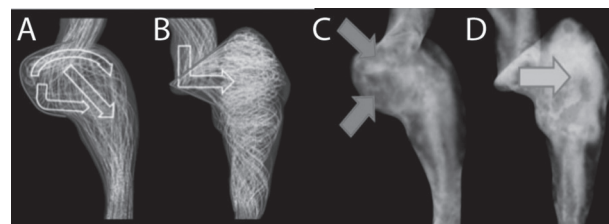
Introduction/purpose Aberrations of venous anatomy can cause pulsatile tinnitus (PT). However, venous anatomy variation in patients without pulsatile tinnitus (PT) is extremely variable. Conventional imaging modalities, including cerebral angiography, provide little insight into the complex flow patterns in the cerebral veins. The aim of this study was to use subject-specific contrast-enhanced MRA (CE-MRA) determined anatomy, and MRV-based inlet flow conditions to develop computational fluid dynamics (CFD) models of flow in subjects with suspected venous pulsatile tinnitus and subjects without pulsatile tinnitus to investigate how the geometry of the jugular vein affects flow.

Materials and methods 7 jugular veins (4 normal, 3 with pulsatile tinnitus) were imaged with CE-MRA. 2 D phase contrast MRV was also acquired transverse to the sigmoid sinus to determine inlet flow conditions. Surfaces were segmented using VMTK (Orobix, Bergamo, Italy) and Geomagic Design X (Geomagic, Rock Hill, USA). Tetrahedral meshing was also performed in VMTK, using a target edge-length of 0.6 mm. CFD simulations were performed in FLUENT (ANSYS, Canonsburg, USA), using flow values obtained from the literature and in vivo measurements. Flow patterns in the jugular vein were characterized by their vortex core-lines, which were extracted from simulation data using Enight (CEI, Apex, USA). Additional flow-parameters were calculated in MATLAB (Mathworks, Natick, USA) and pathlines visualized using Paraview (Kitware, New York, USA).

Results Patients with suspected venous PT had flow distinct patterns from those in normal subjects. Non-PT flow was characterized by organized redirection of flow from the sigmoid sinus along the curvature of the bulb into the jugular vein (A) with vortex cores in the jugular bulb (C). PT flow was characterized by larger helical flow structures throughout the proximal jugular vein created by flow directed

perpendicular to the sigmoid sinus flow (B) and vortex cores that were more diffusely organized (D). High flow rates, and even turbulence, were noted in the proximal jugular vein – near the level of the carotid bifurcation – where there was often pronounced narrowing of the jugular.

Conclusion The geometry of the jugular vein significantly affects the position, size, and length of the vortex cores. Our results suggest a link between geometry, flow, and PT.



Abstract 0-033 Figure 1 Visualization of streamlines (A, B) and vortex cores by swirling strength (C, D) in internal jugular veins of subjects without (A, C) and with (B, D) PT. White arrows (A, B) represent the general re-direction of flow from the sigmoid sinus into the jugular vein as dictated by the shape of the junction with the jugular bulb (red lines). Subjects without PT have strong vortex cores in jugular bulb (C, red arrows), while those with PT have larger, more diffuse vortex cores (D) that encompass nearly the entire proximal jugular vein (blue arrow).

Disclosures E. Kao: None. S. Kefayati: None. K. Meisel: None. M. Ballweber: None. F. Faraji: None. V. Halbach: None. D. Saloner: None. M. Amans: None.

0-034 ABCIXIMAB THERAPY FOR THROMBOEMBOLIC COMPLICATIONS OF NEUROENDOVASCULAR PROCEDURES

¹A Kansagra, ¹T Madaelil, ¹D Cross, III, ¹C Moran, ²C Derdeyn. ¹Washington University School of Medicine, Saint Louis, MO; ²University of Iowa Hospitals and Clinics, Iowa City, IA

10.1136/neurintsurg-2016-012589.34

Background Thromboembolic complications sustained during neuroendovascular procedures can result in postoperative infarcts if not promptly recognized and treated. Treatment commonly involves glycoprotein IIb/IIIa inhibitors such as abciximab. We aimed to retrospectively review angiographic and clinical outcomes following abciximab administration for thromboembolic complications at our institution.

Methods Neuroendovascular cases with thromboembolic complications treated with abciximab over a 132 month period were identified using a search of a comprehensive, prospectively maintained case log and all angiography records for the terms “abciximab” or “ReoPro.” Intraoperative intra-arterial (IA) administration typically involved slow infusion of 10 mg abciximab over 5 to 10 minutes. Intraoperative intravenous (IV) administration 0.25 mg/kg abciximab. Postoperative IV infusion typically involved 10 mcg/min infusion of abciximab. All relevant clinical notes and neuroimaging were reviewed.

Results Of 19,566 neuroendovascular procedures performed during the review period, 48 (0.25%) involved abciximab administration for thromboembolic complications. 65% (31/48) involved IA administration, 21% (10/48) were IV only, and 15% (7/48) were combined IA and IV. Intraoperative treatment was supplemented with postoperative abciximab infusion in 13% (6/48) patients. Angiographic improvement was seen in 92% (44/48) cases, including 65% (31/48) with complete